检 索 证 明

经检索《Science Citation Index Expanded》（SCIE）数据库和《Journal Citation Reports》--- Web of Science 数据库，以下 1 篇文献的收录简要信息、期刊影响因子及分区情况如下：

General model for phase shifting profilometry with an object in motion

作者: Lu, Lei; Yin, Yongkai; Su, Zhilong; 等.

APPLIED OPTICS 卷: 57 期: 36 页: 10364-10369. 出版年: DEC 20 2018

被引频次: 0

(来自 Web of Science 的核心合集)

期刊《APPLIED OPTICS 》2017 年影响因子及分区情况如下：

APPLIED OPTICS

impact factor

1.791 1.755

2017 5 年

JCR ® 类别	类别中的排序	JCR 分区
OPTICS	49/94	Q3

数据来自第 2017 版 Journal Citation Reports

特此证明

（详细内容见附件）

教育部科技查新工作站 Z12

检索人：

2019 年 1 月 3 日

关闭 Web of Science 打印

第 1 页 (记录 1 -- 1)

[1]

第 1 条，共 1 条

标题: General model for phase shifting profilometry with an object in motion

作者: Lu, L (Lu, Lei); Yin, YK (Yin, Yongkai); Su, ZL (Su, Zhilong); Ren, XZ (Ren, Xiaozhen); Luan, YS (Luan, Yinsen); Xi, JT (Xi, Jiangtao)

来源出版物: APPLIED OPTICS **卷:** 57 **期:** 36 **页:** 10364-10369 **DOI:** 10.1364/AO.57.010364 **出版年:** DEC 20 2018

Web of Science 核心合集中的 "被引频次": 0

被引频次合计: 0

使用次数 (最近 180 天): 0

使用次数 (2013 年至今): 0

引用的参考文献数: 15

摘要: When implementing the phase shifting profilometry to reconstruct an object, the object is always required to be kept stable as multiple fringe patterns are required. Movement during the measurement will cause failed reconstruction. This paper proposes a general model describing the fringe patterns with any three-dimensional movement based on phase shifting profilometry. The object movement is classified as five types and their characteristics are analyzed respectively. Then, by introducing a virtual plane, the influence on the phase value caused by different types of movement is described mathematically and a new model including movement information is proposed. At last, with the help of the movement tracking and least-square algorithm, the moving object is reconstructed with high accuracy. The proposed method can remove the reference plane during the reconstruction of the moving object, which extends the application range of the phase shifting profilometry. The effectiveness of the proposed model is verified by the experiments. (C) 2018 Optical Society of America

入藏号: WOS:000453570300002

语言: English

文献类型: Article

KeyWords Plus: PROJECTION; FRINGE; SHAPE; ACCURACY

地址: [Lu, Lei; Ren, Xiaozhen; Luan, Yinsen] Henan Univ Technol, Coll Informat Sci & Engn, Zhengzhou 450001, Henan, Peoples R China.
[Yin, Yongkai] Shandong Univ, Sch Informat Sci & Engn, Jinan 250100, Shandong, Peoples R China.
[Su, Zhilong] Southeast Univ, Sch Civil Engn, Nanjing 210096, Jiangsu, Peoples R China.
[Xi, Jiangtao] Univ Wollongong, Sch Elect Comp & Telecommun Engn, Wollongong, NSW 2522, Australia.

通讯作者地址: Lu, L (通讯作者)， Henan Univ Technol, Coll Informat Sci & Engn, Zhengzhou 450001, Henan, Peoples R China.

电子邮件地址: lulei@haut.edu.cn

出版商: OPTICAL SOC AMER

出版商地址: 2010 MASSACHUSETTS AVE NW, WASHINGTON, DC 20036 USA

Web of Science 类别: Optics

研究方向: Optics

IDS 号: HE6ZI

ISSN: 1559-128X

eISSN: 2155-3165

29 字符的来源出版物名称缩写: APPL OPTICS

ISO 来源出版物缩写: Appl. Optics

来源出版物页码计数: 6

基金资助致谢:

基金资助机构	授权号
National Natural Science Foundation of China (NSFC)	61705060
Science and Technology Department of Henan Province	182102310759

National Natural Science Foundation of China (NSFC) (61705060); Science and Technology Department of Henan Province (182102310759).

输出日期: 2019-01-03

关闭 Web of Science 打印

第 1 页 (记录 1 -- 1)

[1]

applied optics

General model for phase shifting profilometry with an object in motion

Lei Lu,[1,*] Yongkai Yin,[2] Zhilong Su,[3] Xiaozhen Ren,[1] Yinsen Luan,[1] and Jiangtao Xi[4]

[1]College of Information Science and Engineering, Henan University of Technology, Zhengzhou 450001, China
[2]School of Information Science and Engineering, Shandong University, Jinan 250100, China
[3]School of Civil Engineering, Southeast University, Nanjing 210096, China
[4]School of Electrical Computer and Telecommunications Engineering, University of Wollongong, Wollongong, NSW 2522, Australia
*Corresponding author: lulei@haut.edu.cn

Received 10 September 2018; revised 11 November 2018; accepted 11 November 2018; posted 13 November 2018 (Doc. ID 345465); published 11 December 2018

When implementing the phase shifting profilometry to reconstruct an object, the object is always required to be kept stable as multiple fringe patterns are required. Movement during the measurement will cause failed reconstruction. This paper proposes a general model describing the fringe patterns with any three-dimensional movement based on phase shifting profilometry. The object movement is classified as five types and their characteristics are analyzed respectively. Then, by introducing a virtual plane, the influence on the phase value caused by different types of movement is described mathematically and a new model including movement information is proposed. At last, with the help of the movement tracking and least-square algorithm, the moving object is reconstructed with high accuracy. The proposed method can remove the reference plane during the reconstruction of the moving object, which extends the application range of the phase shifting profilometry. The effectiveness of the proposed model is verified by the experiments.

https://doi.org/10.1364/AO.57.010364

1. INTRODUCTION

Phase shifting profilometry (PSP) is one of the most popular techniques for object surface reconstruction [1–5]. Multiple sinusoidal fringe patterns (generated by the laser interference or projector) with phase shifting are projected onto the object surface and the phase information is employed to reconstruct the object. Numerous algorithms are proposed to retrieve the phase information [6–8]. However, since multiple fringe patterns are utilized by the traditional PSP algorithms, the object is required to be kept static. Errors will be introduced when the moving object is measured.

Recently, the methods addressing the errors caused by the movement in PSP attracted intensive attention. Flores *et al.* proposed to reconstruct the object with straight line motion based on PSP [9]. The sinusoidal fringe pattern and homogeneous light pattern in different channels (RGB channel) are projected on the object surface. An iterative algorithm is employed to retrieve the phase information. However, the movement is limited in straight line movement. Liu *et al.* proposed to reduce the motion-introduced phase error by estimating the motion between two subsequent frames [10]. The method assumes the movement speed is constant within the time of capturing two successive 3D frames. However, in practice the assumption may not be satisfied when the speed of projection and capture is low. Feng *et al.* compensated the motion error from three aspects: motion ripples, motion-introduced phase unwrapping errors, and motion outliers [11]. However, the motion-induced phase shifts are assumed to be constant for a single object, leading to the fail when the object with rotation movement is reconstructed. In the author's recent publications, the moving object is reconstructed by analyzing the relationship among the object movement, the phase value on the object, and the phase value on the reference plane [12–14]. At first, the movement is tracked and described mathematically; then, the relationship between the movement, phase value on the object, and the phase value on the reference plane is analyzed; at last, the influence caused by the movement on the phase value is removed and the phase information is retrieved with high accuracy. However, a reference plane is required during the measurement, which limits its applications.

In this paper, a general model for the moving object reconstruction based on phase shifting profilometry is proposed. The reference plane is removed during the measurement. At first, the object movement is classified into five situations and their characteristics are presented. Then, by introducing a virtual plane, the influence caused by the five types of movement on the phase value is analyzed respectively. A general model describing the fringe patterns with movement information is proposed. The real reference plane is not required in the new model. At last, the phase information is

retrieved by the iterative least-square algorithm. Please note that the proposed algorithm is used for the rigid object and the movement includes the translation movement in any direction and rotation movement with the axis perpendicular with the virtual plane.

This paper is organized as follows. Section 2 analyzes the influence on the phase value based on the classification of the movement types. The general model describing the fringe pattern with movement is also presented. In Section 3, an iterative least-square algorithm is described to retrieve the correct phase value based on the general model. Section 4 shows the movement tracking and its mathematics description. Section 5 presents the experimental results to verify the effectiveness of the proposed algorithm. Section 6 concludes this paper.

2. MOVEMENT CLASSIFICATION AND INFLUENCE ON PHASE VALUE

The typical structure for the measurement system employing PSP is shown in Fig. 1. The system includes one camera and one projector. The projector emits the sinusoidal fringe patterns to the object surface and the camera captures the object from another angle. Instead of using the reference plane, a virtual plane is employed to analyze the influence on the phase value caused by the movement. The virtual plane is vertical with the capture direction of the camera and the intensity value of the sinusoidal fringe pattern varies along the x direction. In Fig. 1, the camera captures the fringe patterns from the point A on the object and point B on the virtual plane. As the points A and B are projected by different rays of the fringe patterns, the phase values are also different. The height of the object (distance from A to B) is related to the phase difference between A and B.

A. Classification of the Movement

The object movement is classified as transform movement and rotation movement. The transform movement is further divided into three types based on the relationship between the virtual plane and the movement direction, as shown in Fig. 1. In Fig. 1(a), the movement direction is parallel with the virtual plane. Compared with the virtual plane, the height of the object (AB) does not change with the movement. Therefore, the phase difference between the object and virtual plane is also kept stable. The phase variation caused by the movement is only related to the movement distance along the x direction and all the points on the object have the same variation. In Fig. 1(b), the movement direction is vertical with the virtual plane. Compared with the virtual plane, the entire object is lifted and all the points on the object have the same height variation. Therefore, the corresponding phase variations caused by the movement should also be the same for all the points on the object. Figure 1(c) shows that the movement direction is neither parallel nor vertical with the virtual plane. The movement in Fig. 1(c) is the combination of the movement in Figs. 1(a) and 1(b). Therefore, both of the influences existing in Figs. 1(a) and 1(b) will appear in Fig. 1(c).

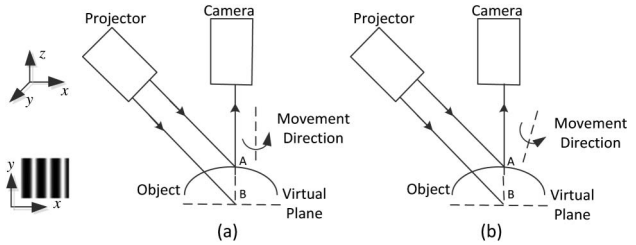

Fig. 2. Measurement system with rotation movement. (a) Measurement system of the rotation movement with the axis vertical with the virtual plane; (b) measurement system of the rotation movement with the axis non-vertical with the virtual plane.

Figure 2 shows the situations when the object has rotation movement. In Fig. 2(a), the object is rotated with the axis which is vertical with the virtual plane. Still use the virtual plane as the reference, the height of the object does not change with the movement. However, a translation movement is introduced for each individual point on the object and different points have different movement distances. In Fig. 2(b), the rotation axis is not vertical with the virtual plane. In this situation, both the position of the object and the height value of each point on the object are changed by the movement. Different from other situations, the height variations are not constant, and different points on the object have different values.

B. Influence Analysis of the Movement

For the traditional PSP, two issues will be introduced when the moving object is reconstructed: (1) the object position among the captured fringe patterns will be mismatched; (2) for the same point on the object, the designed phase shifting value among the fringe patterns will be violated. These issues can be described mathematically as follows.

Assume N-step PSP is used and the captured fringe pattern for the static object can be expressed as

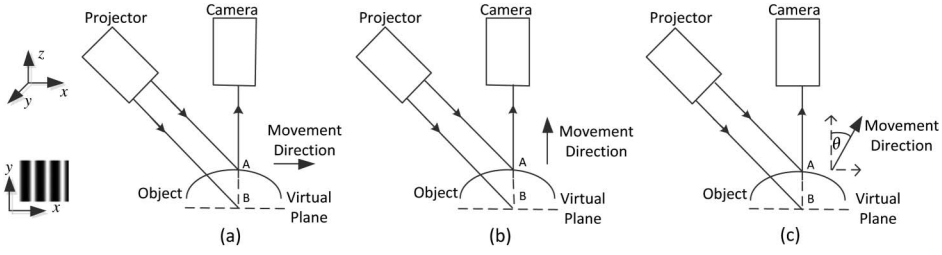

Fig. 1. Measurement system with translation movement. (a) The measurement system with the translation movement in the x direction; (b) the measurement system with the translation movement in the z direction; (c) the measurement system with the translation movement combining Figs. 1(a) and 1(b).

$$d_n(x,y) = a + b\cos[\phi(x,y) + 2\pi n/N] = a + b\cos[2\pi f_0 x + \Phi(x,y) + 2\pi n/N], \quad (1)$$

where $d_n(x,y)$ is the intensity value of the fringe patterns; $n = 1, 2, \ldots, N$ denotes the n-th phase shifting image; a is the background intensity and b is the modulation amplitude; $\phi(x,y)$ is the object phase information to be calculated; f_0 is the frequency of the fringe pattern; and $\Phi(x,y)$ is the phase difference between the object and virtual plane.

A point (x,y) on the object is moved to (ξ,η) and $\xi = f(x,y), \quad \eta = g(x,y)$. $f(\cdot)$ and $g(\cdot)$ are the functions defined by the rotation matrix and translation vector describing the movement. When the object has the movement in Fig. 1(a), the fringe patterns of the object after movement can be described as

$$\tilde{d}_n(\xi,\eta) = a + b\cos[\phi(\xi,\eta) + 2\pi n/N] = a + b\cos[\phi(x,y) + \Delta\Phi^{x-y} + 2\pi n/N], \quad (2)$$

where $\tilde{d}_n(\xi,\eta)$ is the intensity value of the fringe pattern after movement; $\Delta\Phi^{x-y} = 2\pi f_0 \Delta x_c$ is the phase variation caused by the movement in Fig. 1(a); and Δx_c is the movement distance (constant for all the points of the object) along the x direction. As the height of the object keeps constant and only the position of the object is changed by the movement, therefore compared with Eq. (1), the phase value $\phi(x,y)$ does not change and $\Delta\Phi^{x-y}$ is introduced by the movement.

For the movement in Fig. 1(b), only the height of the object is changed by the movement. The fringe pattern after movement can be described as

$$\tilde{d}_n(\xi,\eta) = a + b\cos[\phi(x,y) + \Delta\Phi^{z} + 2\pi n/N], \quad (3)$$

where $\Delta\Phi^{z}$ is the phase variation (constant for all the points of the object) caused by the height variation.

The movement in Fig. 1(c) is the combination of the movement in Figs. 1(a) and 1(b); therefore, we have

$$\tilde{d}_n(\xi,\eta) = a + b\cos[\phi(x,y) + \Delta\Phi^{x-y} + \Delta\Phi^{z} + 2\pi n/N]. \quad (4)$$

From Eqs. (2)–(4) it is clear that, for the translation movement described in Fig. 1, the phase variation caused by the movement is constant for all the points of the object.

The rotation movement in Fig. 2 introduces different influence on the phase value. In Fig. 2(a), the rotation axis is vertical with the virtual plane. For a specific point on the object, the height value does not change with the movement. However, the point has the translation movement in the $x-y$ plane. Furthermore, different points have different translation movements. Therefore, the fringe pattern with the movement in Fig. 2(a) can be expressed as

$$\tilde{d}_n(\xi,\eta) = a + b\cos[\phi(\xi,\eta) + 2\pi n/N] = a + b\cos[\phi(x,y) + \Delta\Phi'^{x-y}(x,y) + 2\pi n/N], \quad (5)$$

where $\Delta\Phi'^{x-y}(x,y) = 2\pi f_0 \Delta x$ is the phase variation caused by the movement in Fig. 2(a) and $\Delta x = \xi - x$ is the movement distance along the x direction. Please note that, different from Eq. (2), $\Delta\Phi'^{x-y}(x,y)$ is not constant for different points on the object.

When the object has the rotation movement in Fig. 2(b), not only the position of the object is shifted in the $x-y$ plane, the height value is also changed by the movement. The fringe pattern with the movement in Fig. 2(b) can be expressed as

$$\tilde{d}_n(\xi,\eta) = a + b\cos[\phi(x,y) + \Delta\Phi'^{x-y}(x,y) + \Delta\Phi'^{z}(x,y) + 2\pi n/N], \quad (6)$$

where $\Delta\Phi'^{z}(x,y)$ is the phase variation caused by the movement on the height direction. Different points on the object have different $\Delta\Phi'^{z}(x,y)$.

Equations (4) and (6) are the expressions describing the fringe patterns with all kinds of translation movement and rotation movement, respectively. Comparing Eqs. (4) and (6), it can be found that $\Delta\Phi^{x-y}$ and $\Delta\Phi^{z}$ are the special cases of $\Delta\Phi'^{x-y}(x,y)$ and $\Delta\Phi'^{z}(x,y)$ when the values are constant among all the points on the object. Therefore, a general model describing the fringe pattern with movement can be obtained as

$$\tilde{d}_n(f_n(x,y), g_n(x,y)) = a + b\cos[\phi(x,y) + 2\pi f_0 \Delta x_n + \Delta\Phi_n'^{z}(x,y) + 2\pi n/N], \quad (7)$$

where $f_1(x,y) = x$, $g_1(x,y) = y$, $\Delta x_1 = 0$, $\Delta\Phi_1'^{z}(x,y) = 0$.

Based on the above derivation, the phase variation caused by the movement can be seen as the phase shifting of the fringe patterns. However, there are some differences between the two situations. First, when the phase variation is introduced by the movement, the object position is mismatched among the multiple fringe patterns and the object tracking algorithm is required. However, when the phase variation is introduced by the phase shifting of the fringe patterns, the object position keeps stable. Second, for the phase variation caused by the phase shifting of the fringe patterns, as the phase shifting is applied to the whole fringe pattern, the phase variation is constant for all the points on the object. On the other hand, for the phase variation caused by the object movement, different points on the object may have different movement distances (such as the movement shown in Fig. 2), leading to the phase variation from point to point.

3. PHASE RETRIEVAL

In Eq. (7), $\tilde{d}_n(f_n(x,y), g_n(x,y))$ can be obtained by the captured fringe patterns; f_0 can be obtained by the calibration of the system [15]. a, b, $\phi(x,y)$ are the same unknown parameters with the ones in traditional methods. Δx_n and $\Delta\Phi'^{z}(x,y)$ are the new unknown parameters introduced by the movement. When the object movement is tracked, the Δx_n can be obtained by comparing the position of the object among the captured images. However, $\Delta\Phi'^{z}(x,y)$ is hard to obtain because the height of the object is an unknown parameter which we need to calculate. Assuming N-step PSP is employed and each fringe pattern has M pixels, we have N equations and MN + 3 unknown parameters in Eq. (7). The phase value is hard to retrieve.

In order to obtain a conclusive result, only the movement in Figs. 1 and 2(a) are considered in this paper. In Figs. 1 and 2(a),

the height variation is constant among all the points on the object. The fringe pattern can be described as

$$\tilde{d}_n(f_n(x,y),g_n(x,y)) = a + b\cos[\phi(x,y) + 2\pi f_0 \Delta x_n + \Delta\Phi_n^z + 2\pi n/N]. \quad (8)$$

Although $\Delta\Phi_n^z$ is still an unknown parameter, it can be seen as the phase shifting error in each fringe pattern. The iterative least-square algorithm described in [8] can be used to retrieve the $\phi(x,y)$.

Step 1: Estimate $\phi(x,y)$ when an estimation of $\Delta\Phi_n^z$ is obtained. The $\Delta\Phi_n^z$ can be seen as zero in the first iteration.

Rewrite Eq. (8) as

$$\tilde{d}_n(f_n(x,y),g_n(x,y)) = a + b\cos[\phi(x,y) + \tau] = a + B(x,y)\cos\tau + C(x,y)\sin\tau, \quad (9)$$

where $\tau = 2\pi f_0 \Delta x_n + \Delta\Phi_n^z + 2\pi n/N$, $B(x,y) = b\cos\phi(x,y)$, and $C(x,y) = -b\sin\phi(x,y)$. Assuming the captured fringe pattern is $\tilde{d}_n^m(x,y)$, the sum of the squared error for each pixel is

$$S(x,y) = \sum_{n=1}^{N}[\tilde{d}_n(f_n(x,y),g_n(x,y)) - \tilde{d}_n^m(x,y)]^2. \quad (10)$$

The phase value is obtained by the least-square algorithm when Eq. (10) is minimized:

$$\phi(x,y) = \tan^{-1}[-C(x,y)/B(x,y)]. \quad (11)$$

Step 2: Estimate $\Delta\Phi_n^z$ with the obtained $\phi(x,y)$ in step 1.

Rewrite Eq. (8) as

$$\tilde{d}_n(f_n(x,y),g_n(x,y)) = a + b\cos[\tau' + \Delta\Phi_n^z] = a + B_n'\cos\tau' + C_n'\sin\tau', \quad (12)$$

where $B_n' = b\cos\Delta\Phi_n^z$, $C_n' = -b\sin\Delta\Phi_n^z$, and $\tau' = \phi(x,y) + 2\pi f_0 \Delta x_n + 2\pi n/N$. The sum of the squares error in each frame is

$$S_n' = \sum_{(x,y)}[\tilde{d}_n(f_n(x,y),g_n(x,y)) - \tilde{d}_n^m(x,y)]^2. \quad (13)$$

Similar with step 1, the least-squares algorithm is applied to minimizing S_n', then $\Delta\Phi_n^z$ can be obtained by

$$\Delta\Phi_n^z = \tan^{-1}[-C_n'/B_n']. \quad (14)$$

Repeat step 1 and step 2 until the convergence condition in Eq. (15) is satisfied:

$$|(\Delta\Phi_n^{zk} - \Delta\Phi_1^{zk}) - (\Delta\Phi_n^{zk-1} - \Delta\Phi_1^{zk-1})| < \varepsilon, \quad (15)$$

where k is the iteration times and ε is the accuracy requirement, e.g., 10^{-4}. The detailed description can be found in [8].

4. MOVEMENT TRACKING AND MATHEMATICAL DESCRIPTION

In order to implement the above phase retrieval algorithm, the method proposed in [12] is employed to track the object movement and calculate the rotation matrix and translation vector describing the movement. A color camera is required, and the red fringe patterns are projected. The fringe pattern information can be found in the red component of the captured image. In the blue component of the captured image, a pure object image can be obtained as the red fringe patterns are "filtered out." Then, the scale-invariant feature transform algorithm is implemented to track the object movement based on the pure object image. The corresponding points between the object before movement and after movement are also obtained. At last, the singular value decomposition method is used to calculate the rotation matrix and translation vector.

Assume $\{\mathbf{p}_i | i = 1,\ldots,N\}$ are the feature points of the object before movement and $\{\mathbf{q}_i | i = 1,\ldots,N\}$ are the corresponding points of the object after movement. N is the number of the corresponding point pairs and i is the number index. The movement is described by the rotation matrix and translation vector as the following:

$$\mathbf{q}_i = \mathbf{R}\mathbf{p}_i + \mathbf{T} + \boldsymbol{\gamma}_i, \quad (16)$$

where $\mathbf{R}$ is the rotation matrix, $\mathbf{T}$ is the translation vector, and $\boldsymbol{\gamma}_i$ is a noise vector. $\mathbf{R}$ and $\mathbf{T}$ can be obtained by minimizing Eq. (17):

$$\sum{}^2 = \sum_{i=1}^{N}\|\mathbf{q}_i - (\mathbf{R}\mathbf{p}_i + \mathbf{T})\|^2. \quad (17)$$

Define

$$\mathbf{p}' = \frac{1}{N}\sum_{i=1}^{N}\mathbf{p}_i, \qquad \mathbf{p}_i'' = \mathbf{p}_i - \mathbf{p}'. \quad (18)$$

$$\mathbf{q}' = \frac{1}{N}\sum_{i=1}^{N}\mathbf{q}_i, \qquad \mathbf{q}_i'' = \mathbf{q}_i - \mathbf{q}'. \quad (19)$$

Then we have

$$\sum{}^2 = \sum_{i=1}^{N}\|\mathbf{q}_i'' - \mathbf{R}\mathbf{p}_i''\|^2. \quad (20)$$

Therefore, the estimated value for the rotation matrix $\hat{\mathbf{R}}$ can be obtained by minimizing $\sum^2$ in Eq. (20); the estimated value for the translation vector $\hat{\mathbf{T}}$ is calculated by $\hat{\mathbf{T}} = \mathbf{q}' - \hat{\mathbf{R}}\mathbf{p}'$.

Define the 3×3 matrix $\mathbf{H}$ as

$$\mathbf{H} = \sum_{i=1}^{N}\mathbf{p}_i''\mathbf{q}_i''^T. \quad (21)$$

Using the singular value decomposition algorithm to obtain $\mathbf{H} = \mathbf{U}\Lambda\mathbf{V}^T$, the optimal rotation matrix $\hat{\mathbf{R}}$ can be obtained by the following:

(a) (b)

Fig. 3. Mask used in the experiment. (a) The mask used in the experiment; (b) the captured red fringe patterns of the object.

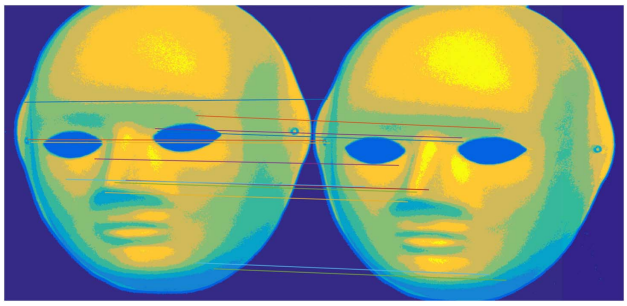

Fig. 4. Object tracking result with the image in blue component when the object has rotation movement.

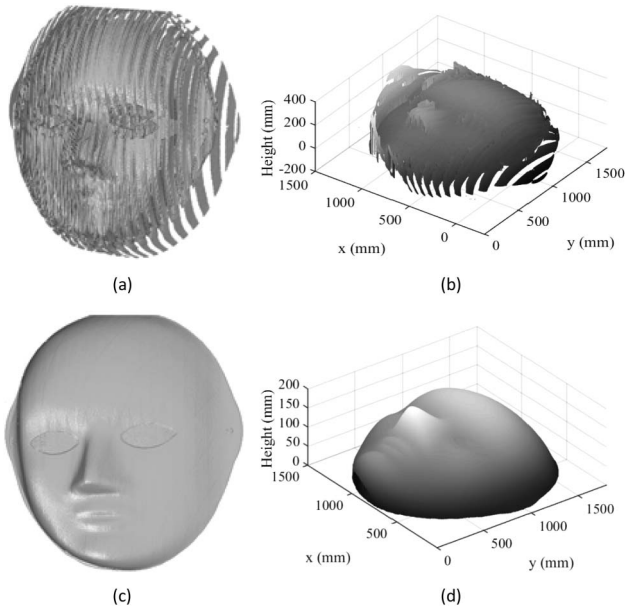

Fig. 5. Reconstructed results with the traditional PSP and the proposed algorithm. (a) The front view of the result with the traditional PSP; (b) the mesh display of Fig. 5(a); (c) the front view of the result with the proposed algorithm; (d) the mesh display of Fig. 5(c).

$$\hat{\mathbf{R}} = \mathbf{V}\mathbf{U}^T, \tag{22}$$

and the translation vector is determined as

$$\hat{\mathbf{T}} = \mathbf{q}' - \hat{\mathbf{R}}\mathbf{p}'. \tag{23}$$

5. EXPERIMENTS

As the proposed method is not sensitive to the movement, this paper employs five-step PSP to verify the effectiveness of the proposed method. A mask shown in Fig. 3(a) is moved randomly in three-dimension during the measurement [except the movement in Fig. 2(b)]. In the first experiment, the object is moved in the directions of x, y, z, and clockwise rotation, respectively, from the first fringe pattern to the fifth fringe pattern. In order to retrieve the movement information, the method described in [12] is used to track the object. The red fringe patterns as shown in Fig. 3(b) are projected onto the object surface and a color camera is used to capture the object with movement. The red channel of the captured image (with the fringe pattern information) is used to reconstruct the object and the blue channel (with the object movement information) is used to track the movement. Figure 4 shows the tracking result when the object has rotation movement.

The object is reconstructed with the traditional PSP algorithm and the proposed algorithm, respectively. The results are shown in Fig. 5. The results obtained by the traditional PSP are shown in Figs. 5(a) and 5(b). It is apparent that significant errors are introduced by the movement. Figures 5(c) and 5(d) show the results of the proposed approach. The object is reconstructed well, and the errors caused by the movement are removed.

In the second experiment, the movements in Figs. 1 and 2(a) are completed separately to evaluate the performance of the proposed method. The results are shown in Fig. 6. The first row shows the reconstruction results based on the traditional PSP with the movement in Figs. 1(a)–1(c) and 2(a), respectively. The second row shows the corresponding results based on the proposed algorithm.

In order to evaluate the accuracy performance of the proposed method quantitatively, the above experiment results

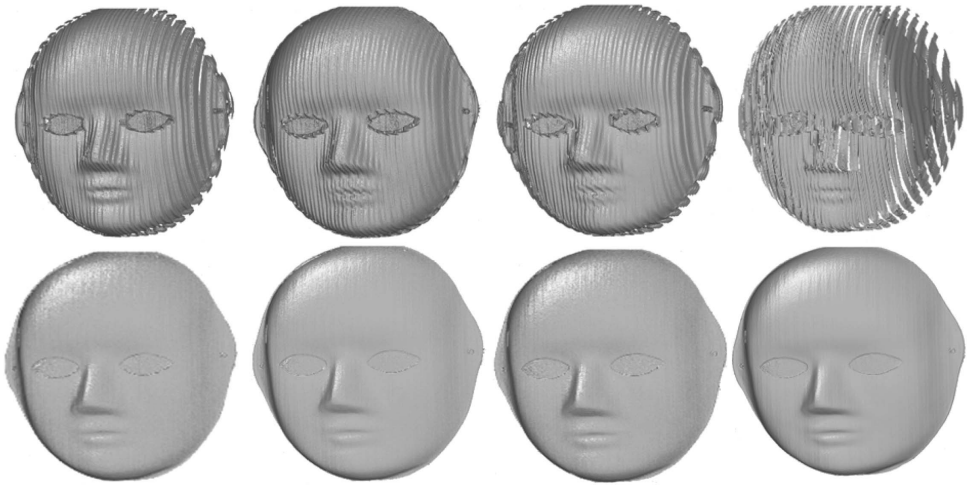

Fig. 6. Reconstructed results with the traditional PSP and the proposed algorithm for the movement in Figs. 1 and 2(a).

Table 1. Comparison Results Between the Traditional PSP and the Proposed Method

Movement Type	RMS Error (Traditional PSP)	RMS Error (Proposed Method)	Number of the Iteration Cycles
Movement in Fig. 1(a)	45.912 mm	0.083 mm	7
Movement in Fig. 1(b)	35.491 mm	0.079 mm	6
Movement in Fig. 1(c)	55. 682 mm	0.084 mm	7
Movement in Fig. 2(a)	87.993 mm	0.089 mm	7
Combination movement in Fig. 5	72.381 mm	0.087 mm	8

are compared with the result obtained by the traditional PSP when the object is stable. The comparison results are shown in Table 1. The root mean square (RMS) measurement error is reduced significantly with the proposed method. In our experiment, the number of the iteration cycles is less than 10.

6. CONCLUSION

This paper proposes a general model for the moving object reconstruction based on phase shifting profilometry. The reference plane is removed when the moving object is reconstructed with high accuracy. The object movement is classified into five situations and the characteristics for each type of the movement are analyzed. Then, by introducing a virtual plane, the influence on the phase distribution caused by the different types of the movement is described mathematically and a new model describing the fringe pattern of the object with any three-dimensional movement is proposed. At last, the object is reconstructed successfully by the iterative least-square algorithm. The object is limited in rigid shape and the rotation movement whose axis is non-vertical with the virtual plane is excluded. With the proposed method, the reference plane is not required during the measurement, which extends the application range of the phase shifting profilometry.

Funding. National Natural Science Foundation of China (NSFC) (61705060); Science and Technology Department of Henan Province (182102310759).

REFERENCES

1. S. Zhang, D. Weide, and J. Oliver, "Superfast phase-shifting method for 3-D shape measurement," Opt. Express **18**, 9684–9689 (2010).
2. Y. Xing, C. Quan, and C. Tay, "A modified phase-coding method for absolute phase retrieval," Opt. Lasers Eng. **87**, 97–102 (2016).
3. H. Cui, W. Liao, N. Dai, and X. Cheng, "Reliability-guided phase-unwrapping algorithm for the measurement of discontinuous three-dimensional objects," Opt. Eng. **50**, 063602 (2011).
4. A. Babaei, M. Saadatseresht, and J. Kofman, "Exponential fringe pattern projection approach to gamma-independent phase computation without calibration for gamma nonlinearity in 3D optical metrology," Opt. Express **25**, 24927–24938 (2017).
5. Y. Liu, Q. Zhang, and X. Su, "3D shape from phase errors by using binary fringe with multi-step phase-shift technique," Opt. Lasers Eng. **74**, 22–27 (2015).
6. C. Zuo, S. Feng, L. Huang, T. Tao, W. Yin, and Q. Chen, "Phase shifting algorithms for fringe projection profilometry: a review," Opt. Lasers Eng. **109**, 23–59 (2018).
7. S. Zhang, "High-speed 3D shape measurement with structured light methods: a review," Opt. Lasers Eng. **106**, 119–131 (2018).
8. Z. Wang and B. Han, "Advanced iterative algorithm for phase extraction of randomly phase-shifted interferograms," Opt. Lett. **29**, 1671–1673 (2004).
9. J. L. Flores, G. Ayubi, J. Martino, O. Castillo, and J. Ferrari, "3D-shape of objects with straight line-motion by simultaneous projection of color coded patterns," Opt. Commun. **414**, 185–190 (2018).
10. Z. Liu, P. Zibley, and S. Zhang, "Motion-induced error compensation for phase shifting profilometry," Opt. Express **26**, 12632–12637 (2018).
11. S. Feng, C. Zuo, T. Tao, M. Zhang, Q. Chen, and G. Gu, "Robust dynamic 3-D measurements with motion-compensated phase-shifting profilometry," Opt. Lasers Eng. **103**, 127–138 (2018).
12. L. Lu, Y. Ding, Y. Luan, Y. Yin, Q. Liu, and J. Xi, "Automated approach for the surface profile measurement of moving objects based on PSP," Opt. Express **25**, 32120–32131 (2017).
13. L. Lu, J. Xi, Y. Yu, and Q. Guo, "New approach to improve the accuracy of 3-D shape measurement of moving object using phase shifting profilometry," Opt. Express **21**, 30610–30622 (2013).
14. L. Lu, J. Xi, Y. Yu, and Q. Guo, "Improving the accuracy performance of phase-shifting profilometry for the measurement of objects in motion," Opt. Lett. **39**, 6715–6718 (2014).
15. Z. Huang, J. Xi, Y. Yu, Q. Guo, and L. Song, "Improved geometrical model of fringe projection profilometry," Opt. Express **22**, 32220–32232 (2014).